Recombination dynamics of Landau levels in an InGaAs/InP quantum well

M. D. Teodoro,[1] B. G. M. Tavares,[2] E. D. Guarin Castro,[1] R. R. LaPierre,[3] and Yu. A. Pusep[2]
[1]*Departamento de Física, Universidade Federal de São Carlos, 13565-905, São Carlos, São Paulo, Brazil*
[2]*São Carlos Institute of Physics, University of São Paulo, P.O. Box 369, 13560-970 São Carlos, SP, Brazil*
[3]*Centre for Emerging Device Technologies, Department of Engineering Physics, McMaster University, Hamilton, Ontario, Canada L8S 4L7*

(Received 17 August 2018; revised manuscript received 4 October 2018; published 22 October 2018)

The dynamics of differently spin-polarized carriers photoexcited in a system of Landau levels is investigated in an InGaAs/InP quantum well. Shake-up emission from Landau levels above the Fermi level is observed, and it is shown to significantly affect the recombination dynamics of Landau levels. The shake-up effect is found to occur due to the inter-Landau-level scattering, which manifests itself in a rapid decay of the emission from Landau levels. In addition, the inter-Landau-level scattering is shown to determine the time delay of photoluminescence response due to the relaxation of photoexcited electrons among Landau levels. The sharp minimum of the recombination time is observed between the quantum Hall phases with the filling factors $\nu = 1$ and 2, and it is attributed to the formation of the metallic intermediate phase, which causes increasing overlap between the electron and hole wave functions.

DOI: 10.1103/PhysRevB.98.155431

I. INTRODUCTION

The advantage of the spectroscopic method is that it probes the electron states below (photoluminescence) and above (photoluminescence excitation measurements, absorption) the Fermi energy, while the electronic states in close vicinity of the Fermi surface are responsible for the electric transport. As a result, the photoluminescence (PL) emission of the two-dimensional electron gas (2DEG) subjected to a perpendicular quantizing magnetic field directly reveals its fundamental feature—Landau quantization in the form of the number of PL lines (Landau level fan chart), each corresponding to an appropriate Landau level (LL). Thus, the energy distribution of the one-particle density of states below and above the Fermi energy, the characteristic band-gap energy, and the broadening of the electron states involved in the recombination process may be determined. Moreover, the time evolution of the electron states may be studied by time-resolved PL. At an appropriately high magnetic field/mobility, the LL states develop into quantized Hall states corresponding to the incompressible quantum Hall liquids (Hall insulator), which are manifested as the quantized plateau Hall resistance $R_{xy} = h/\nu e^2$, where ν is the integer LL filling factor. A varying magnetic field changes the filling factor, resulting in a quantum phase transition between the quantized Hall states. Such a transition is caused by the quantum percolation process and it takes place continuously in the intermediate metallic phase related to the magnetic field range where the Hall resistance changes between two neighboring plateaus [1–4].

In the regime of the quantum Hall effect, several phenomena are responsible for the optical response of the 2DEG, which causes changes in the energy, intensity, and broadening of observed PL lines. These phenomena were explored in a broad range of different heterostructures. A corresponding comprehensive review, which includes the effects due to magnetic field modulation of the screening efficiency and exchange-enhanced spin-splitting, is presented in Ref. [5]. The PL intensity and the line broadening expose magneto-oscillations caused by oscillations in the one-particle density-of-states width as a function of filling factor [6]. In addition, the PL emission energy and line broadening were shown to oscillate with the magnetic field due to the screening of the impurity binding energy [7–9]. Furthermore, due to the fact that in the quantum Hall regime, as the filling factor changes, a sequence of the metal-Hall insulator transitions takes place, the PL energy might also change as a result of band-gap renormalization [10,11] and screening of free excitons [12]. The metal-Hall insulator transition manifests itself in the PL spectra as a corresponding variation of the line intensity and width. The PL line becomes narrower, and as a consequence larger in intensity in the metallic phase due to the screening effect. Moreover, a supplementary manifestation of the metal-Hall insulator transition can be found in the corresponding variation of the recombination time. In general, the probability of the transition between the initial $|i\rangle$ and final $\langle f|$ eigenstates relates to the overlap integral of the corresponding wave functions and to the density of states according to the Fermi golden rule:

$$\frac{1}{\tau} = \frac{2\pi}{\hbar}|\langle f|H|i\rangle|^2\rho_f, \tag{1}$$

where H is the interaction Hamiltonian, which couples the initial and final states, and ρ_f is the density of the final states. Therefore, the recombination time τ is fundamentally defined by the nature of the electron states involved in the transition. Consequently, a drastic change in the recombination time is expected when the transition between quantized Hall phases occurs.

To the best of our knowledge, only a few time-resolved PL experiments in the quantum Hall regime have been reported to date. The time evolution of optical recombination was first studied in a high-mobility GaAs/AlGaAs single quantum well in Ref. [13], where a sharp increase of the radiative recombination time was found at the filling factor $\nu = 1$ and it was explained as an effect of localization and changes in the screening response of the electrons. Similar results were obtained in the regime of the fractional quantum Hall effect in Ref. [14]. Time-resolved magneto-PL was examined in a GaAs/AlAs multiple quantum well [15]. The observed rise of the recombination time above the filling factor $\nu = 2$ was attributed to the magnetic-field-induced Mott metal-insulator transition. The dynamics of inter-LL excitations using time-resolved nonlinear spectroscopy was studied in a GaAs/AlGaAs multiple quantum well in Ref. [16] where a large transfer of oscillator strength to the lowest LL caused by shake-up of the electron gas was observed. It is worth mentioning that no combination of time- and polarization-resolved measurements in the quantum Hall regime have been reported so far. Optical polarization enables spectroscopic separation of the spin-split electron states. However, most of the results cited above were obtained in GaAs-based heterostructures where the optical study of spin effects is difficult due to the small electron g factor responsible for the spin splitting. In this way, InGaAs-based heterostructures are of particular interest because of the value $g = -5$, which is much larger as compared to $g = -0.44$ in GaAs [17]. Thus, it is expected that in InGaAs-based heterostructures, the spin polarization may dominate over the Coulomb energy effects in a high magnetic field, resulting in a response of the electron system different from that observed in GaAs.

In the present study, we employ time-resolved magneto-PL to probe the transition between the quantized Hall phases around the filling factors $\nu = 1$ and 2 in an InGaAs/InP quantum well. The PL emission transients with different circular polarizations are analyzed, which was not achieved in the previously cited works. The previously reported oscillations of the ground-state LL energy in GaAs quantum wells caused by the filling-factor-dependent screening effect are observed. Moreover, the InGaAs/InP quantum well studied here reveals different dynamic responses of LLs: (i) shake-up emission from LLs above the Fermi level is observed, and it is found to significantly affect the recombination dynamics of the ground-state LL; (ii) the sharp minimum of the recombination time is found in the interval of the external magnetic field where the transition between the quantum Hall phases with the filling factors $\nu = 1$ and 2 takes place; the recombination time minimum is attributed to the formation of the metallic intermediate phase. In addition, evidence of the insignificant role of spin-flip effects is demonstrated.

II. EXPERIMENTAL DETAILS

An $In_xGa_{1-x}As$/InP single quantum well with lattice-matched composition $x = 0.53$ was grown on (100)-oriented InP substrates by a gas source molecular beam epitaxy system. Before growing the structure, a 150 nm wide InP buffer layer was deposited. On the top of the buffer layer, the 10 nm wide $In_{0.53}Ga_{0.47}As$ quantum well was grown followed by a 20 nm wide InP undoped spacer separating the quantum well and dopant Si atoms and by a 5 nm InP layer doped with Si doping density of 2.2×10^{12} cm^{-2}. Finally, a 44 nm wide InP layer was grown on the top of the structure. Such a one-sided doping results in an asymmetric potential energy profile of the quantum well.

PL, time-resolved PL, and magnetotransport measurements were performed at 4 K using a home-made confocal microscope, mounted on top of a vibration-free helium closed-cycle cryostat (Attocube-Attodry 1000). The samples were pumped by a diode laser (PicoQuant–LDH 1080) emitting at 1080 nm both in a continuous wave (CW) and in a pulsed mode at the frequency of 40 MHz. A fixed circular polarization was achieved by setting a linear polarizer and a corresponding quarter wave plate in front of the sample, while a change in the circular polarization was accomplished by a corresponding change in the magnetic-field orientation. In our experimental conditions, the positive/negative magnetic field corresponded to the σ^+/σ^- circular polarization, respectively. Circularly polarized PL was analyzed using a 50 cm Andor-Shamrock spectrometer. CW emission was measured by an InGaAs diode array Andor-DU491A detector, while PL transients were measured using a time-correlated single-photon counting procedure (PicoQuant-PicoHarp 300) with the signal detected by an H10330B-75 Hamamatsu infrared photomultiplier tube. The electron densities and the mobilities obtained by standard Hall measurements at 4 K with a pump power density 6 μW/μm^2 were $n = 2.3 \times 10^{11}$ cm^{-2} and $\mu = 1.6 \times 10^4$ cm^2/V s, respectively. At such an electron concentration, only the lowest conduction-band miniband is populated.

III. RESULTS AND DISCUSSION

The magnetotransport traces obtained with the pumping power used during the PL measurements are shown in Fig. 1. The distinct quantum Hall states corresponding to the filling factors $\nu = 1$ and 2 were found at magnetic fields of 8 and 4 T, respectively. These data are used to determine the filling-factor scale used in the following.

The PL spectra measured as a function of the magnetic field with different circular polarizations are shown in Fig. 2. For each polarization with increasing magnetic field a zero-field broad PL emission splits into distinct lines corresponding

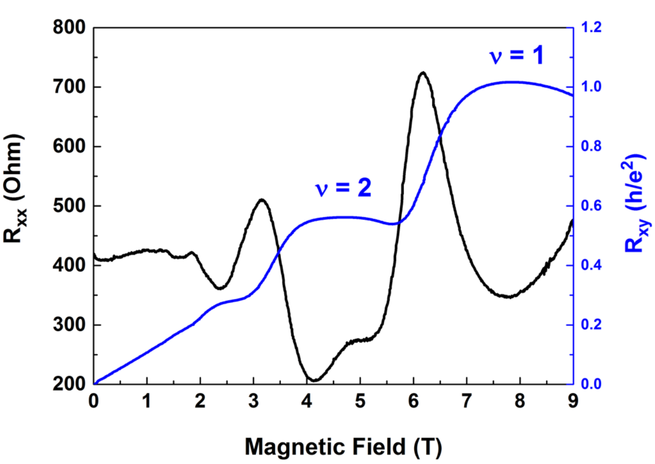

FIG. 1. Magnetoresistance traces measured in an $In_{0.53}Ga_{0.47}As$/InP quantum well at temperature 4 K.

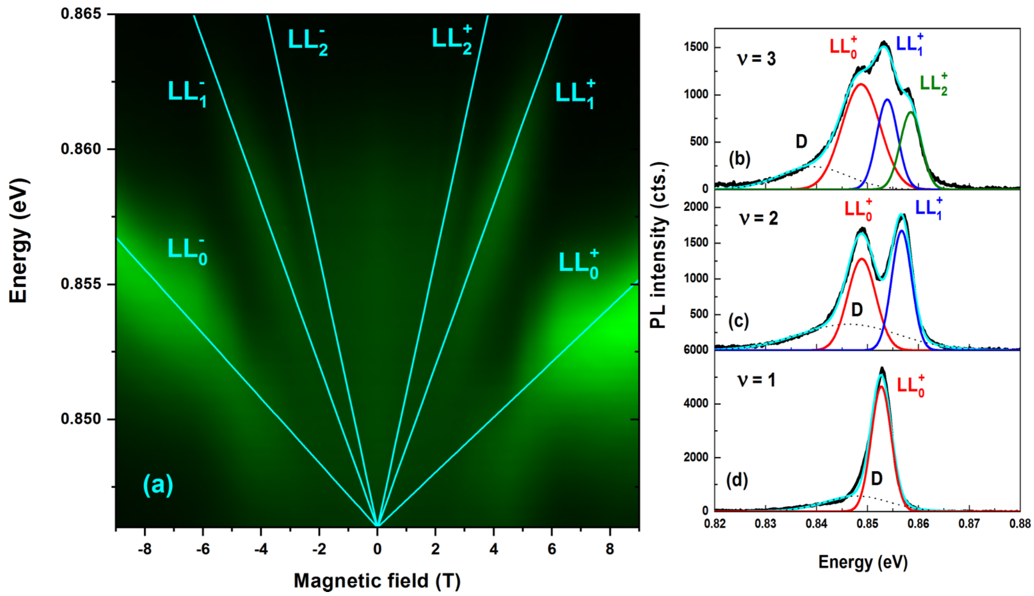

FIG. 2. Photoluminescence spectra measured in an $In_{0.53}Ga_{0.47}As/InP$ quantum well at temperature 4 K. (a) The positive and negative magnetic field correspond to σ^+ and σ^- circular polarization, respectively; the calculated energies of the corresponding Landau levels are shown by cyan lines. Panels (b), (c), and (d) show the details of the photoluminescence spectra measured at different filling factors (ν). A defect-related PL emission (D) is shown as the dashed line.

to LLs. The fits with the Gaussian lines were performed in order to determine spectroscopic characteristics (peak position, integral intensity, and broadening) of the emissions from LLs. The results of the fits are shown in Figs. 2(b)–2(d) for the magnetic fields corresponding to the filling factors $\nu = 1, 2, 3$.

In addition to the PL lines due to LLs, a broad line designated as D line was observed and assigned to emission due to defects. The following arguments point to the defect origin of the D line: (i) it contributes to the lowest-energy band tail of the PL emission; (ii) the energy separation of the D-line from the lowest energy LL does not change with the magnetic field and it is estimated to be about 5 meV, which is close to the expected ionization energy of shallow impurities; and (iii) the intensity of the D-line (shown in Fig. 4) does not depend on the magnetic field. However, we have no available information about what kind of defects form the D line. The intensity of the D line is much less than the corresponding intensities of the observed LLs. Therefore, the D line was not considered in the analysis of the LL dynamics presented below.

The PL peak energies related to LLs are shown in Fig. 3, where the Landau level energies calculated according to one-particle interband transitions are shown by broken lines. The best fit of the calculated LL energies to the energies of the corresponding PL peaks was obtained with the exciton effective mass $m_{\mathrm{exc}} = 0.052$, which is in reasonable agreement with the exciton effective masses $m_{\mathrm{exc}} = 0.031m_0$ and $0.046m_0$ reported in InGaAs/InP [18] and in InGaAs/GaAs quantum wells [19], respectively.

Considerable oscillations of the energy are observed for the ground state LL_0. It is commonly accepted that the oscillations of the LL energy correlating with the filling factor are due to the filling-factor-dependent screening effect [5,8,9,20,21]: completely filled or empty LLs do not screen the Coulomb interaction. Therefore, bare excitons are observed in the Hall insulator phases corresponding to integer filling factors, while in the intermediate metallic phases free electron screening results in a screened reduced exciton binding energy. Such an oscillatory screening accounts for the oscillations of the ground state LL_0 energy shown in Fig. 3.

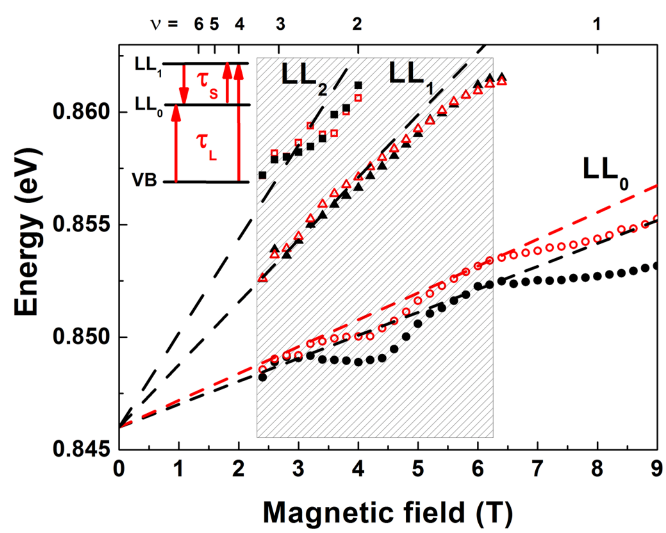

FIG. 3. The fan chart of the emission energies from Landau levels in an $In_{0.53}Ga_{0.47}As/InP$ quantum well at 4 K. Closed and open symbols correspond to σ^+ and σ^- circular polarization, respectively; the calculated Landau level energies are shown by broken lines. The shaded area demonstrates the magnetic field range where the shake-up excitations contribute to the emission from the quantum well. The inset depicts the relevant energy structure of the quantum well where the transitions related to the minority carriers (holes) with the short τ_S and long τ_L characteristic times are shown.

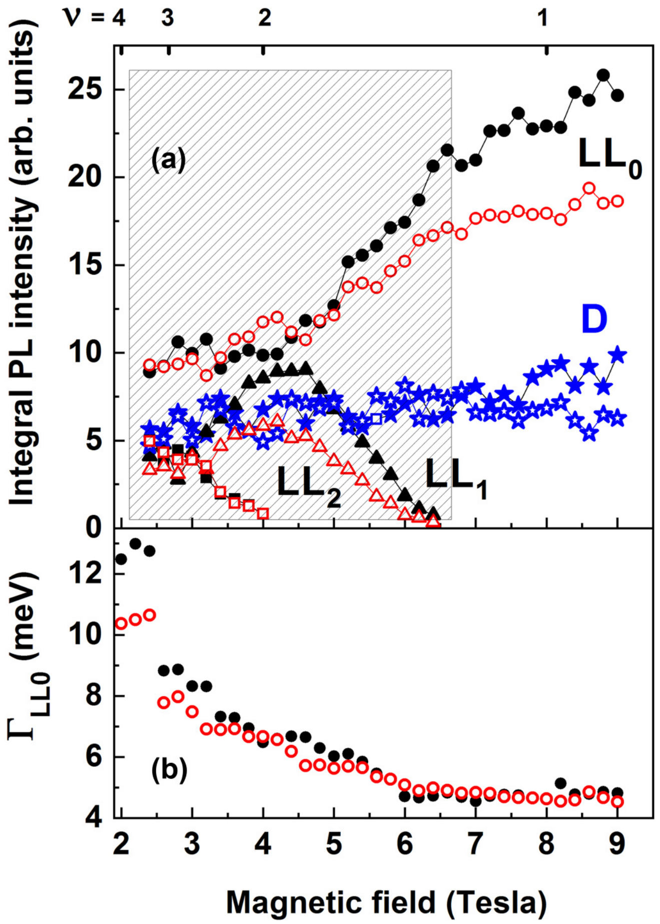

FIG. 4. (a) Integrated photoluminescence intensities of the emissions from Landau levels, and (b) full width at half maximum (FWHM) of the PL line attributed to ground state LL_0 measured as a function of the magnetic field in an $In_{0.53}Ga_{0.47}As/InP$ quantum well at 4 K. The shaded area in panel (a) demonstrates the magnetic field range where the shake-up excitations contribute to the emission from the quantum well. Closed and open symbols correspond to σ^+ and σ^- circular polarization, respectively.

The spin splitting of the ground state LL_0 corresponds to the exciton g factor equal to -3.53.

The evolution of the LLs occupancy with increasing magnetic field is depicted in Fig. 4(a). As expected, the integral intensity of the PL emission D associated with defects does not reveal any noteworthy change with the magnetic field, while LLs are consequently depopulated with increasing magnetic field. The number of emitting LLs was more than the related filling factor, which points to the presence of the shake-up process [18,22]. The shake-up excitation manifests itself in an additional electron-hole pair excited in the system of the Fermi electrons, which causes a partial occupancy of the LLs above the Fermi level [21,23]. The magnetic field range where the shake-up process contributes to the observed PL is indicated in Figs. 3 and 4(a) by the shaded area. In the magnetic field above this range, the lowest ground state LL_0 is found in both polarizations with almost the same intensities. Moreover, depopulation of LLs with the same quantum number but different polarization takes place at the same magnetic field value. The observed insensitivity of the LL depopulation on the optical polarization indicates two independent recombination channels of differently spin-polarized photoexcited carriers, and as a consequence, a negligible spin-flip process in the InGaAs/InP quantum well studied here.

It is worth mentioning that the filling-factor-dependent screening may also cause magnetic-field-induced oscillations of the width of the PL line due to the LL. However, as follows from Fig. 4(b), no such oscillations are observed in the broadening of the emission from the ground state LL_0, which was found to decrease monotonically with increasing magnetic field. An absence of such oscillatory behavior is likely due to the dominant contribution of disorder to the LL broadening, which masks the screening effect.

The most important results obtained in this study are related to the time-resolved PL experiments. In our recent work [24], we demonstrated that localization of excitons is closely related to localization of electrons in the conduction band of an n-doped semiconductor heterostructure. To be precise, the random potential yields inhomogeneous broadening of excitons, which makes electrons and holes localize in different regions due to their different charges. Thus the overlap integral of the electron and hole wave functions decreases, leading to the increasing recombination time according to Eq. (1). In Ref. [24], we found that the exciton recombination time in a disordered electron system reveals all the features expected in the case of localized electrons.

The σ^- PL transients measured in different magnetic fields are shown in Fig. 5. Similar results are obtained in σ^+ circular polarization. As is presented in Figs. 5(a) and 5(c), in low and high magnetic fields a monoexponential decay with the characteristic time τ_L accounts for the observed PL transients, while in the interval of the magnetic field corresponding to the filling factor around $\nu = 2$ shown in Fig. 5(b), the fits of the PL transients were obtained with two characteristic times: short τ_S and long τ_L. The two-exponential decay is even more pronounced in the case of the recombination due to the excited LL_1. Two recombination times point to the presence of two groups of photogenerated carriers that recombine independently. To explain the observed LL dynamics, we employ a three-level model shown in the inset of Fig. 3, which takes into account the transitions between the valence band LLs (not shown) and the conduction band ground state LL_0 and first-excited LL_1. Such transitions are governed by the kinetics of the minority carriers, which in our case of the n-doped quantum well are the photogenerated holes in the valence band (VB). In addition, the transitions between LL_0 and LL_1 due to the inter-LL electron-electron scattering are also considered. The observed short and long recombination times are attributed to the inter-LL transitions and to the interband transitions, respectively. In this case, following Ref. [25], the recombination dynamics of the ground-state LL_0 can be described by the rate equations:

$$\frac{dp_{\rm VB}}{dt} = -\frac{p_{\rm VB}}{\tau_L}, \quad \frac{dp_1}{dt} = -\frac{p_1}{\tau_S}, \tag{2}$$

while similar rate equations account for the recombination dynamics of the first-excited LL_1:

$$\frac{dp_{\rm VB}}{dt} = -\frac{p_{\rm VB}}{\tau_L}, \quad \frac{dp_0}{dt} = -\frac{p_0}{\tau_S}, \tag{3}$$

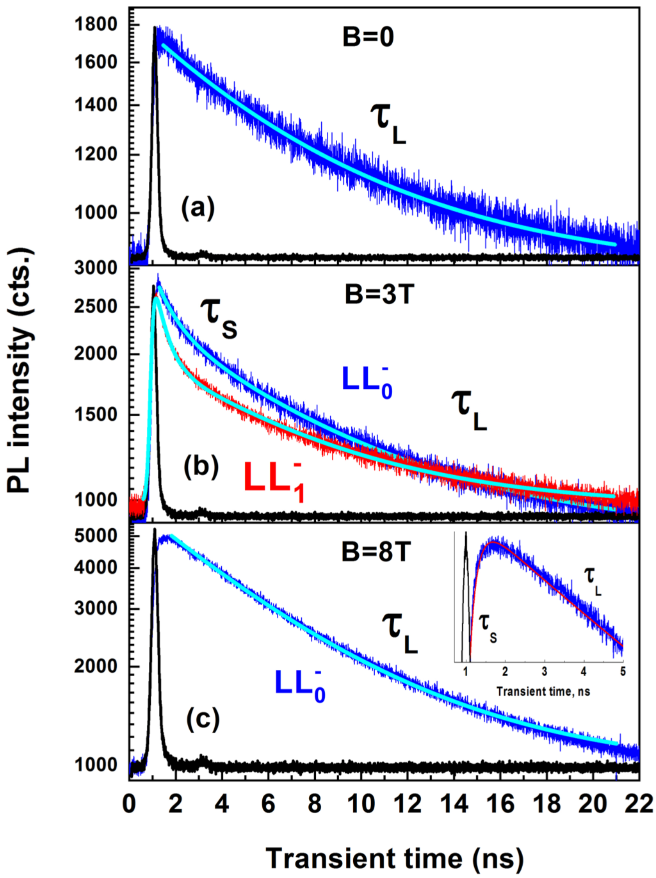

FIG. 5. Photoluminescence transients measured in zero magnetic field (a) and in different magnetic fields (b),(c) in an $In_{0.53}Ga_{0.47}As/InP$ quantum well at 4 K. Thin cyan lines show the results of the best fits as explained in the text, while black line represents the internal response function (IRF) of the equipment. The inset to the panel (c) shows enlarged PL intensity decay.

where p_{VB}, p_0, and p_1 are the hole concentration in the valence band, on the ground LL_0, and on the first-excited LL_1, respectively, while τ_S and τ_L are the characteristic transition times corresponding to the inter-LL scattering and intraband recombination processes, respectively. Equation (2) describes the recombination of the electrons on LL_0 with the holes in the valence band and on LL_1, while Eq. (3) gives an account of the recombination of the electrons on LL_1 with the holes in the valence band and on LL_0. In both cases, the inter-LL scattering is responsible for the transitions between the LLs. Equations (1) and (2) show that two independent channels with corresponding characteristic times τ_S and τ_L contribute to the recombination of the electrons residing on the LLs. Based on Eqs. (2) and (3), we derive the temporal decay of the PL intensity:

$$I_{PL}(t) = A_S e^{-\frac{t}{\tau_S}} + A_L e^{-\frac{t}{\tau_L}}, \tag{4}$$

where $A_{S(L)}$ is the PL amplitude corresponding to the short τ_S and long τ_L times, respectively.

Furthermore, the PL transients due to LL_0 reveal a significant delay increasing with increasing magnetic field. No such delay is found in the case of the zero-magnetic-field transient shown in Fig. 5(a) and for the decay of the PL due to LL_1. The inset to Fig. 5(c) depicts an enlarged transient scale, where the delay of the LL_0 PL transient is clearly observed. The observed delay is likely caused by relaxation of the photoexcited electrons among LLs. The laser excitation first pumps the excited LL_1, and then the population of LL_0 from LL_1 takes place. Therefore, the population of LL_0 first increases, resulting in increasing PL intensity. The PL intensity decays after the LL_0 filling becomes larger than its depopulation due to recombination processes. In such a case, according to [25], the population of the low-energy LL_0 state can be expressed as a function of time as

$$n_0(t) \sim (e^{-t/\tau_L} - e^{-t/\tau_S}), \tag{5}$$

where we assume that the filling of LL_0 from LL_1 takes place with the characteristic time τ_S, which is essentially the inter-LL scattering time. Thus, our experimental data provide two ways to determine the short inter-LL scattering time: first, using the delay of the PL response of the LL_0, and second, employing transients due to LL_0 and LL_1. It should be mentioned that the LL_0 time-delay response was clearly observed in the magnetic field higher than 6 T, when the separation between the LLs is large enough.

We used the PL intensity decay proportional to $n_0(t)$ in order to fit the LL_0 PL transients measured in a high magnetic field. The result of such a fit for the case of the magnetic field 8 T performed with the times $\tau_S = 0.2$ ns and $\tau_L = 9$ ns is shown in the inset to Fig. 5(c). The short recombination time τ_S obtained in the interval of the magnetic field 6–9 T where the LL_0 delay is mostly visible is shown in Fig. 6(b).

Two recombination times τ_S and τ_L obtained by the fits of the PL intensity decay calculated by Eq. (4) to the PL intensity transients due to LL_0 and LL_1 measured as a function of the magnetic field in two circular polarizations are shown in Fig. 6.

The overall drop of the long LL_0 recombination time with increasing magnetic field is caused by the corresponding rise in the LL density of states. As already established above, two recombination times account for the PL intensity decays from LL_0 and LL_1 in the range of the filling factor around $\nu = 2$, where both LLs contribute to the PL. In this range, the population of LL_1 due to the inter-LL scattering is considerable. In higher magnetic field, the energy separation between LLs grows, leading to the suppression of the inter-Landau scattering. Consequently, a decreasing population of LL_1 makes it invisible in PL measurements. However, even in such a case LL_1 contributes to the filling of LL_0 resulting in a time delay. The value of the short lifetime determined by the fit of the time-delayed LL_0 PL transients is in reasonable agreement with the short recombination time obtained by the fit of the PL intensity decay. This is consistent with our assumption that the observed time delay originates from the filling of the LL_0 from LL_1, and the characteristic inter-LL transition time defines both processes: the inter-LL scattering and the filling of the LL_0 from LL_1.

A well defined drop in the LL_0 long recombination time and in the LL_1 short recombination time indicated by arrows in Fig. 6 is found in the magnetic field corresponding to the metallic phase between the filling factors $\nu = 2$ and 1. In the metallic phase, the overlap between the electron

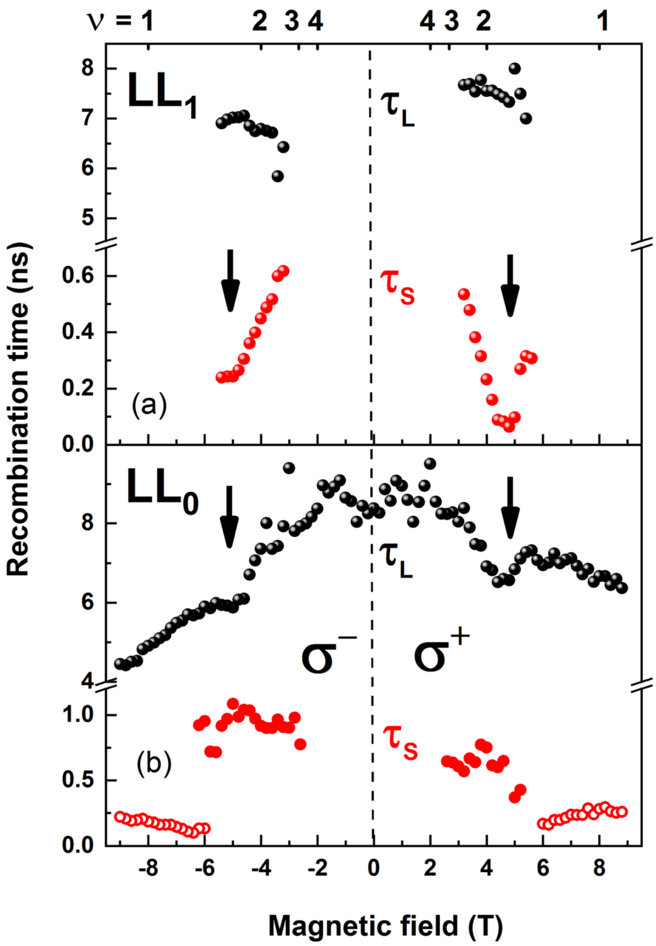

FIG. 6. Recombination times obtained by the fits of the PL intensity transients due to ground state LL_0 and excited state LL_1 measured as a function of the magnetic field in two circular polarizations for the $In_{0.53}Ga_{0.47}As/InP$ quantum well. The open circles correspond to the short recombination time τ_S obtained by the fit of the LL_0 time delay.

and hole wave functions increases, which leads to a faster recombination according to Eq. (1). Such a performance of the recombination time is different from that observed in Ref. [13], where a sharp increase of the recombination time was found in the insulating phase at exact filling factor $\nu = 1$. As is demonstrated in Fig. 6, a similar behavior of the recombination times is observed in both circular polarizations. It should be mentioned that the obtained recombination time τ_L yields the total lifetime, which involves both the radiative and nonradiative characteristic times. Determination of individual radiative and nonradiative contributions is beyond the scope of this study.

IV. CONCLUSION

The dynamics of differently spin-polarized photoexcited carriers was investigated in a system of Landau levels formed in an InGaAs/InP quantum well. Oscillations of the ground state Landau level energy caused by the filling-factor-dependent screening of excitons were observed in both spin-up and spin-down polarizations. The obtained results are evidence of an insignificant spin-flip process in the InGaAs/InP quantum well. Shake-up emission from Landau levels above the Fermi level was observed, and it was found to considerably affect the recombination dynamics of Landau levels. Specifically, the inter-Landau-level scattering responsible for the shake-up effect manifests itself in a rapid decay of the emission from Landau levels. The same inter-Landau-level scattering is shown to determine the time delay of photoluminescence response due to the relaxation of photoexcited electrons among Landau levels. The characteristic time of about 200 ps of the inter-Landau-level transitions was determined. The sharp minimum of the recombination time was found in the interval of the magnetic field where the transition between the quantum Hall phases with the filling factors $\nu = 1$ and 2 takes place; the recombination time minimum is attributed to the formation of the metallic intermediate phase, which causes increasing overlap between the electron and hole wave functions.

ACKNOWLEDGMENTS

Financial support from the Brazilian agencies FAPESP, CNPq, CAPES, and the Natural Science and Engineering Research Council of Canada is gratefully acknowledged.

[1] D. C. Tsui and S. J. Allen, Jr., Phys. Rev. B **24**, 4082 (1981).
[2] R. F. Kazarinov and S. Luryi, Phys. Rev. B **25**, 7626 (1982).
[3] S. Kivelson, D.-H. Lee, and S.-C. Zhang, Phys. Rev. B **46**, 2223 (1992).
[4] D.-H. Lee, Z. Wang, and S. Kivelson, Phys. Rev. Lett. **70**, 4130 (1993).
[5] I. V. Kukushkin and V. B. Timofeev, Adv. Phys. **45**, 147 (1996).
[6] T. Ando, J. Phys. Soc. Jpn. **43**, 1616 (1977).
[7] K. Meimberg, M. Potemski, P. Hawrylak, Y. H. Zhang, and K. Ploog, Phys. Rev. B **55**, 7685 (1997).
[8] M. Potemski, Physica B **256-258**, 283 (1998).
[9] A. Raymond, B. Couzinet, M. I. Elmezouar, M. Kupisa, W. Zawadski, and B. Etienne, Europhys. Lett. **43**, 337 (1998).
[10] S. Katayama and T. Ando, Solid State Commun. **70**, 97 (1989).
[11] T. Uenoyama and L. J. Sham, Phys. Rev. Lett. **65**, 1048 (1990).
[12] D. C. Reynolds, D. C. Look, and B. Jogai, J. Appl. Phys. **88**, 5760 (2000).
[13] M. Dahl, D. Heiman, A. Pinczuk, B. B. Goldberg, L. N. Pfeiffer, and K. W. West, Phys. Rev. B **45**, 6957 (1992).
[14] D. Heiman, A. Pinczuk, H. Okamura, M. Dahl, B. S. Dennis, L. N. Pfeiffer, and K. W. West, Physica B **201**, 315 (1994).
[15] H. W. Yoon, M. D. Sturge, and L. N. Pfeiffer, Solid State Commun. **104**, 287 (1997).
[16] N. A. Fromer, C. E. Lai, D. S. Chemla, I. E. Perakis, D. Driscoll, and A. C. Gossard, Phys. Rev. Lett. **89**, 067401 (2002).
[17] H. Kosaka, A. A. Kiselev, F. A. Baron, K. W. Kim, and E. Yablonovitch, Electron. Lett. **37**, 464 (2001).

[18] Yu. A. Pusep, M. A. Tito, and R. R. LaPierre, J. Phys. Condens. Matter **28**, 175602 (2016).

[19] K.-S. Lee, C.-D. Lee, Y. Kim, and S. K. Noh, Solid State Commun. **128**, 177 (2003).

[20] T. Ando and Y. Uemura, J. Phys. Soc. Jpn. **37**, 1044 (1974).

[21] K. Asano and T. Ando, Phys. Rev. B **65**, 115330 (2002).

[22] Yu. A. Pusep, L. F. dos Santos, G. M. Gusev, D. Smirnov, and A. K. Bakarov, Phys. Rev. Lett. **109**, 046802 (2012).

[23] K. J. Nash, M. S. Skolnick, M. K. Saker, and S. J. Bass, Phys. Rev. Lett. **70**, 3115 (1993).

[24] M. A. Tito and Yu. A. Pusep, Phys. Rev. B **97**, 184203 (2018).

[25] G. Bastard, *Wave Mechanics Applied to Semiconductor Heterostructures* (Halsted, New York, 1988).